the resulting V_{sg} curve is flatter in the middle region where both NMOS and PMOS are in triode mode; and it is sharper when Vtune is either low or high where either NMOS or PMOS is in saturation mode, respectively. With this characteristic, this voltage converter not only extends the linear region of varactor's C-V curve, but also reduces its noise contribution to the VCO.

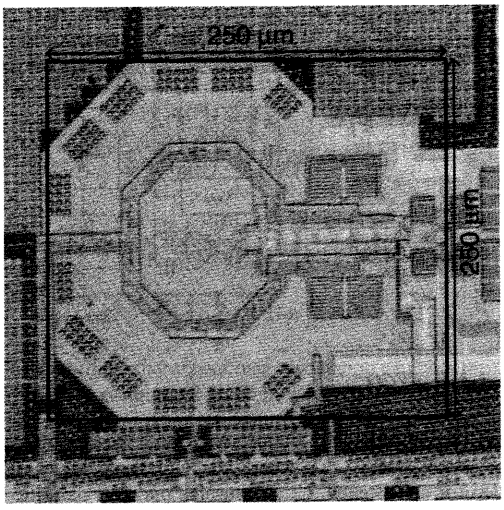

Fig. 3 *Die photo of VCO core*

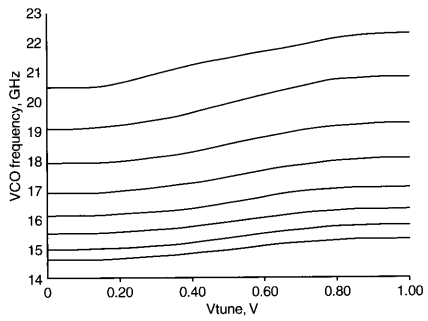

Fig. 4 *Measured VCO frequency against control voltage*

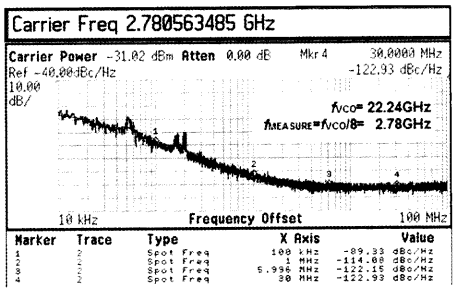

Fig. 5 *Measured phase noise profile at VCO frequency of 22.2 GHz*

Fig. 2 also shows the C-V curve from one NMOS varactor with differential and single-ended tuning schemes. The differential scheme has a C_{max}/C_{min} of 4.9, 30% larger than that of the single-ended scheme. Even in the presence of parasitic capacitance that decreases the tuning range, simulation shows that the overall FTR of the VCO is increased by 7–8% by using the differential approach over its single-ended counterpart.

Measurement results: The VCO is fabricated in TSMC 65 nm 1P6M GP CMOS process. Fig. 3 shows the die photo of the VCO core. It occupies an area of 250 by 250 μm, including the guard-ring of the inductor. The core of the VCO consumes 2.6 mW under a 0.65 V supply. Fig. 4 shows the measured VCO F-V characteristics. They cover the entire 14.6–22.3 GHz frequency range with sufficient overlap between adjacent bands. At the highest oscillation frequency, the VCO exhibits the worst phase noise of −96 dBc/sqrt(Hz) at 1 MHz offset. To compensate for the effects of the divide-by-8 circuit embedded in the test driver, 18 dB is added to the measured phase noise shown in Fig. 5.

Conclusion: We present a VCO implemented in 65 nm CMOS technology. By employing a differential tuning scheme enabled by a simple voltage amplifier, the VCO achieves 14.6–22.3 GHz FTR. For ultra-wideband applications that need a carrier frequency from 50 MHz to 10 GHz, the upper octave range of 5–10 GHz can be provided by this VCO with subsequent divide-by-2 and 3 circuits, and all other lower frequency carriers can be generated by further cascading a number of divide-by-2 circuits as needed.

7 February 2011
doi: 10.1049/el.2011.0348
One or more of the Figures in this Letter are available in colour online.

J. Lu, N.-Y. Wang and M.-C.F. Chang (*Department of Electrical Engineering, University of California, Los Angeles, California 90095, USA*)

E-mail: jianhua@ucla.edu

References

1 Razavi, B.: 'Multi-decade carrier generation for cognitive radios'. IEEE VLSI Circuits Symp. Dig., Kyoto, Japan, June 2009, pp. 120–121
2 Soorapanth, T., *et al.*: 'Analysis and optimization of accumulation-mode varactor for RF ICs'. Symp. on VLSI Circuits, Honolulu, HI, USA, 1998, pp. 33–34
3 Osmany, S.A., *et al.*: 'Integrated 22 GHz low-phase-noise VCO with digital tuning in SiGe BiCMOS technology', *Electron. Lett.*, 2009, **45**, (1), pp. 39–40

Frequency synthesis chain for ESA deep space network

S. Grop, P.-Y. Bourgeois, E. Rubiola, W. Schäfer, J. De Vicente, Y. Kersalé and V. Giordano

A report is presented on the measurement of a frequency synthesiser that provides round frequencies (10 GHz, 5 MHz, 100 MHz) with high spectral purity from a cryocooled sapphire oscillator in the vicinity of 10 GHz. The synthesiser and sapphire oscillator are a part of Elisa, a frequency reference that exhibits a stability of parts in 10^{-15} from 1 s to 1000 s integration time, designed and implemented for the European Space Agency. The synthesiser features low $1/f$ phase noise, −96 dBc/Hz at 1 Hz off the carrier at the 10 GHz output, and −133 dBc/Hz at 1 Hz offset at the 100 MHz output.

Introduction: Since the early time of space exploration, it has been known that whenever a new technology provides a better oscillator or clock, it enables several applications already in the list [1, 2]. This general principle originated Elisa, a precision oscillator built around a cryocooled sapphire and intended to provide a reliable 10 GHz reference signal with stability $\sigma_y(\tau) = 3 \times 10^{-15}$ (Allan deviation) for measurement time $\tau = 1 \ldots 10^3$ s and the lowest possible phase noise. The prototype outperformed the specs, providing higher stability and extending the full-stability τ to at least 10^5 s [3] and exhibiting a phase noise of −101 dBc at 1 Hz offset frequency [4].

System architecture: The system architecture derives from the need of keeping far from the paramagnetic resonance of sapphire impurities, 11.35 GHz for Cr^{3+} and 12.4 GHz for Fe^{3+}, and from the fact that only a chain of dividers can provide sufficiently low noise at the 100 MHz output. The best frequencies were 12.8 and 10.0 GHz, and 10.0 GHz won only for practical reasons. Yet, unlike the quartz resonator, the sapphire cannot be machined precisely at the exact desired frequency. The minimum tolerance is of a few MHz, far beyond the tuning range. A synthesiser is therefore necessary.

Given the 10^{-15} stability at 10 GHz, the appropriate resolution is in the μHz range. This can only be provided by a 48 bit DDS. Yet the DDS, not designed for metrology, can spoil the phase noise. While the DDS phase noise is in general proportional to the output frequency, it turns out that the noise of this device below $\simeq$20 MHz is limited by

the output stage. This issue is well known in the frequency divider [5]. If the frequency offset $\Delta\nu$ provided by the synthesiser is smaller than $\simeq$20 MHz, the sapphire-oscillator purity is preserved. A minimum $\Delta\nu$ of a few MHz prevents the sapphire signal leaking into the 10 GHz output, while $\Delta\nu = 5$ MHz and $\Delta\nu = 10$ MHz must be avoided because of highly coherent 5–10 MHz signals present in the machine may have unpredictable effects.

The cost of this strategy is that precision modelling and machining the resonator are critical issues. The resonator and synthesiser are designed together because the oscillation frequency must differ from 10 GHz by $\Delta\nu = \pm 12.5 \pm 2$ MHz or $\Delta\nu = \pm 7.5 \pm 2$ MHz. The benefit is that the machine is easily reproducible, and that the synthesiser is dramatically simplified. It is only thanks to the high stability that derives from simplicity, that the unexpected beyond-specs stability of the oscillator could be transferred to the output.

Synthesiser architecture: The block diagram of the Elisa synthesiser is shown in Fig. 1. The 10.0 GHz main signal is obtained by mixing the oscillator output with the $\Delta\nu$ DDS frequency, after cleaning with a PLL. The clean-up is necessary because the frequency offset $\Delta\nu$ is low, $\simeq$10 MHz. The Analog Devices AD9854 48-bit DDS clocked at 250 MHz provides a resolution of 0.89 μHz, thus 8.9×10^{-17} at 10 GHz. The PLL bandwidth is $\simeq$20 kHz. The DRO frequency is 2.5 GHz, chosen because DROs exhibit the highest stability in this range. Very few DROs are stable enough to achieve 10^{-15} in closed loop. The 100 MHz output is obtained by direct division of the 10 GHz output with Hittite dividers.

Results: We evaluate the synthesiser by comparing two equal units with the scheme of Fig. 2. Alizé is an oscillator similar to Elisa, but in a liquid-He cryostat instead of the pulse-tube cooler. The phase comparators (PCOs) phase-lock the two outputs (10 GHz or 100 MHz) to the H maser by acting on the DDS control word with a time constant of 300 s. This guarantees the quadrature in the long run, but leaves the two synthesisers free to fluctuate. We cannot drive the two synthesisers with a single oscillator because all frequencies would be the same, and in turn the noise would be underestimated by the effect of leakage. The results are shown in Figs. 3 and 4.

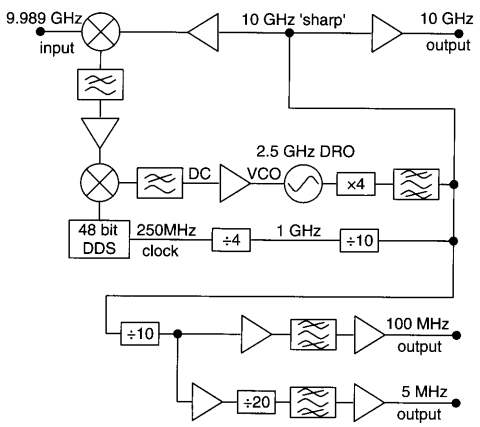

Fig. 1 *Block diagram of Elisa synthesiser*

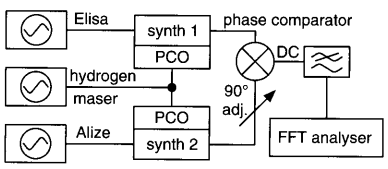

Fig. 2 *Phase noise measurement*

At the 10 GHz output flicker (−96 dBc at 1 Hz) is the dominant process. A bump at 300 Hz is clearly visible, owing to the Pound frequency lock of the oscillator, and a smaller bump at $\simeq$20 kHz owing to the DRO PLL inside the synthesiser. The residual of the Pound phase modulation shows up just below 100 kHz. The modulation frequency is intentionally different for the two oscillators. The 1.14 Hz vibration of the pulse-tube cooler is well identified. Another vibration shows up at 11 Hz, likely a mechanical resonance powered by the pulse tube. Though disturbing, these artifacts have virtually no effect on the Allan deviation at $\tau > 1$ s. The $1/f^3$ broken line is the frequency-flicker floor $\sigma_y(\tau) = 2 \times 10^{-15}$, which is the stability of Elisa and Alizé at $\tau = 1 \ldots 100$ s. In the absence of noise in the frequency division, the phase noise spectrum at the 100 MHz output is exactly that of the noise at 10 GHz, lowered by 40 dB. Looking at Fig. 4, most phenomena are as predicted. Beyond $f = 500$ Hz, the white noise of the divider output stage sets the minimum noise. This hides the effect of the DRO PLL. Below $f = 0.5$ Hz, the spectrum seems to be limited by the frequency flicker, shown as the broken line on the left-hand side. The phase flicker (−133 dBc at $f = 1$ Hz) is ascribed to the frequency dividers from 10 GHz to 100 MHz. The value is consistent with the measurement of such devices, and marginally acceptable as compared to specs. To this extent, it is pointed out that the phase flicker yields a $1/(\tau\sqrt{\ln\tau})$ law in the Allan deviation, which in our case has negligible effect on the Allan deviation at $\tau = 1$ s and beyond. Thanks to electrical simplicity, this synthesiser outperforms the earlier SYRTE design [6].

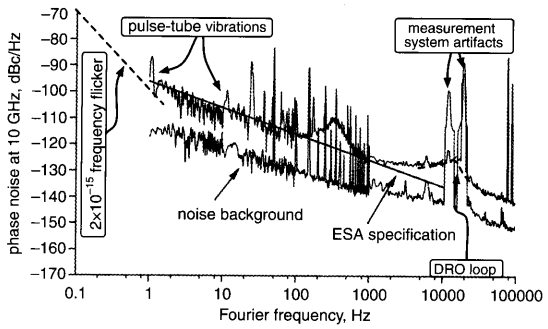

Fig. 3 *Phase noise of one synthesiser measured at 10 GHz output*

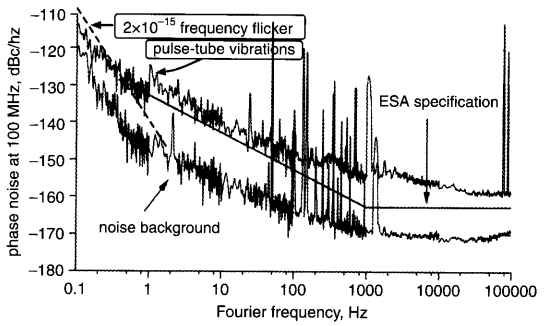

Fig. 4 *Phase noise of one synthesiser measured at 100 MHz output*

Conclusion: We have developed a frequency synthesiser for the European Space Agency with residual phase noise of −96 and −133 dBc/Hz at 1 Hz offset frequency from the carrier at 10 GHz and 100 MHz, respectively. This synthesiser, associated with the cryo-cooled sapphire oscillator, will be installed in the Cebreros (Spain) ESA ground base station.

4 January 2011
doi: 10.1049/el.2011.0028

S. Grop, P.-Y. Bourgeois, E. Rubiola, Y. Kersalé and V. Giordano (*Time and Frequency Dept., FEMTO-ST Institut, UMR 6174 CNRS – ENSMM, Besançon 25044, France*)

E-mail: yann.kersale@femto-st.fr

W. Schäfer (*TimeTech GmbH, Curiestrasse 2, Stuttgart D-70563, Germany*)

J. De Vicente (*European Space Agency ESA-ESOC, Robert Bosch Str. 5, Darmstadt D-64293, Germany*)

References

1 Develet, J.: 'Fundamental accuracy limitations in a two way coherent Doppler measurement system', *IRE Trans. Space Electron. Telemetry*, 1961, **SET-7**, (3), pp. 80–85

2 Thornton, C.L., and Border, J.S.: 'Radiometric tracking techniques for deep space navigation' (Wiley and Sons, 2003)
3 Grop, S., Bourgeois, P.-Y., Basin, N., Kersale, Y., Rubiola, E., Langham, C., Oxborrow, M., Clapton, D., Walker, S., Vicente, J.De, and Giordano, V.: 'ELISA: a cryocooled 10 GHz oscillator with 1e-15 frequency stability', *Rev. Sci. Instrum.*, 2010, **81**, p. 025102
4 Grop, S., Bourgeois, P.-Y., Boudot, R., Kersale, Y., Rubiola, E., and Giordano, V.: '10 GHz cryocooled sapphire oscillator with extremely low phase noise', *Electron. Lett.*, 2010, **46**, (6), pp. 420–422
5 Egan, W.F.: 'Modeling phase noise in frequency dividers', *IEEE Trans. Ultrason. Ferroelectr. Freq. Control*, 1990, **37**, (4), pp. 307–315
6 Chambon, D., Bize, S., Lours, M., Narbonneau, F., Marion, H., Clairon, A., Santarelli, G., Luiten, A.N., and Tobar, M.E.: 'Design and realization of a flywheel oscillator for advanced time and frequency metrology', *Rev. Sci. Instrum.*, 2005, **76**, p. 094704

Triple-mode bandpass filter using defected ground waveguide

H.W. Liu, L. Shen, Y. Jiang, X.H. Guan, S. Wang, L.Y. Shi and D. Ahn

A novel triple-mode bandpass filter using an open-loop slotline resonator in a defected ground waveguide is presented. Distinct characteristics of the triple-mode resonator are investigated by using even-odd mode analysis. The proposed filter has been designed, fabricated and measured. Good agreement between simulation and measurement verifies the validity of this design methodology.

Introduction: Multi-band microwave components with compact sizes and low cost are now required and have been studied. Microstrip dual-mode resonators and filters have been the subject of intensive research efforts. These include square-loop resonators, meander-loop resonators and stepped-impedance resonators (SIRs) [1–4]. Also, multimode filters in metal waveguide technology have been known for some time [5]. However, they tend to be heavy, expensive, and occupy a large volume.

In [6], a defected ground waveguide (DGW) structure was reported; it is compact and easily integrable with planar technology. In this Letter, a novel defected open-loop resonator in slotline configuration is applied to design a compact triple-mode DGW resonator and bandpass filter (BPF). Characteristics of the triple-mode resonator are investigated using even-odd mode analysis. Simulated and measured results are given.

Triple-mode BPF design using DGW: A schematic view of the proposed triple-mode BPF using a DGW resonator is shown in Fig. 1. This BPF consists of two layers. On the bottom layer for slotline configuration, a half-wavelength ($\lambda/2$) open-loop DGW resonator is etched on the backside metallic ground plane [6]. Another two defected T-shape stubs are tapped from outside and inside of the open loop. The dimension parameters of this slotline resonator are denoted by L_2–L_8 and the slot width is s. On the top layer, there is a pair of L-shaped microstrip I/O feed lines. The microstrip feed line is described by W_1 and L_1. The circuits on different layers enclosed within dashed lines are overlapped to provide broadside coupling. The substrate has a thickness $h = 0.8$ mm and a relative dielectric constant $\varepsilon_r = 4.5$ in this work.

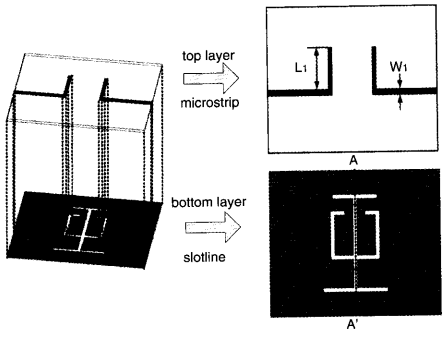

Fig. 1 *Schematic view of triple-mode BPF using DGW*

Similar to the even-odd mode analysis for a microstrip open-loop resonator [4], the fundamental resonant frequency (named Odd mode) of this DGW resonator may be determined by the defected open-loop resonator itself. Furthermore, another two resonant frequencies (named Even mode I and Even mode II) may be adjusted by the two defected T-shape stubs. For demonstration purpose, this tri-mode DGW resonator is simulated by Ansoft HFSS 10 and the electric field distributions of these modes are presented in Fig. 2. It is interestingly found that the odd mode has a field distribution similar to that of the singlemode open-loop DGW resonator. Hence, the tapping point of the loading element is actually a virtual ground for the odd mode. As a consequence, the loading elements affect the odd-mode characteristics slightly. However, a significant field distribution is seen within the loading elements for two even modes. Thus, the two loading elements result in shifting the even-mode frequencies for triple-mode operation. Resonant characteristics of the triple-mode slotline resonator with different stub lengths (L_4 and L_7) are compared. The results, shown in Fig. 3, prove that the defected stubs can greatly adjust the two even modes whereas it has slight effect on the odd mode location.

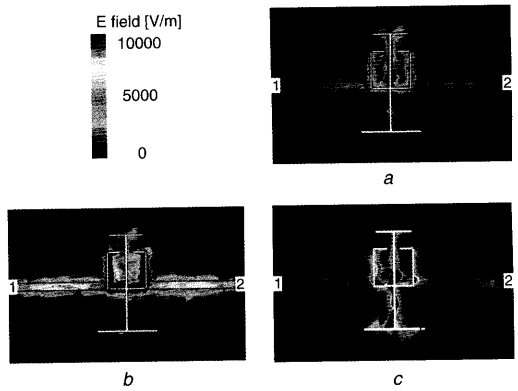

Fig. 2 *Electric field distributions for triple-mode DGW resonator*
a Even mode I (at 3.25 GHz)
b Odd mode (at 3.56 GHz)
c Even mode II (at 3.78 GHz)

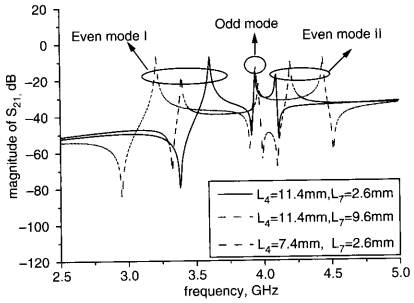

Fig. 3 *Resonant characteristics of triple-mode DGW resonator*

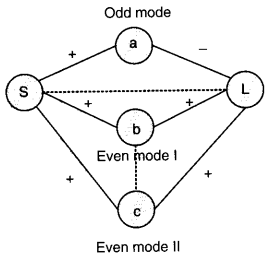

Fig. 4 *Coupling schematic of proposed filter*

The coupling and routing scheme is applied to model the operation of this triple-mode slotline resonator, shown in Fig. 4. The circles a, b, c represent the three modes and the circles S and L represent the input and output, respectively. The input and output are coupled to the modes by the admittance inverters, which are represented by the solid lines. There is no coupling between the even modes and odd mode. In addition, the input and output are weakly coupled, denoted by the dashed line. Synthesis of such a coupling scheme follows the approach in [7]. The triple-mode filter has a centre frequency of 3.5 GHz, a bandwidth of 560 MHz, and three attenuation poles at $-0.9242j$, $0.2118j$,